Chinese Chemical Letters 34 (2023) 108069

Contents lists available at ScienceDirect

Chinese Chemical Letters

journal homepage: www.elsevier.com/locate/cclet

Build in seconds: Small-molecule hydrogels of self-assembled tryptophan derivatives

Xianwen Song[a,1], Jun Zheng[a,1], Shunmei He[a], Yilin Liu[b], Shutong Yang[a], Qiang Li[a], Chuntai Liu[c], Zequn Zhang[d], Xi Liu[d], Chunyan Deng[a,*], Yi Zhang[a,*]

[a] Hunan Provincial Key Laboratory of Micro & Nano Materials Interface Science, College of Chemistry and Chemical Engineering, Central South University, Changsha 410083, China
[b] Beijing National Laboratory for Molecular Sciences (BNLMS), CAS Key Lab of Colloid, Interface and Chemical Thermodynamics Institute of Chemistry, Chinese Academy of Sciences, Beijing 100190, China
[c] Key Laboratory of Materials Processing and Mold (Zhengzhou University), Ministry of Education, Zhengzhou 450002, China
[d] Department of Gastrointestinal Surgery, The Third Xiangya Hospital of Central South University, Changsha 410013, China

ARTICLE INFO

Article history:
Received 30 August 2022
Revised 24 November 2022
Accepted 12 December 2022
Available online 14 December 2022

Keywords:
Small-molecule
Hydrogel
Tryptophan derivatives
Self-assemble
Self-healing
Density functional theory

ABSTRACT

Small-molecule hydrogels based on amino acid derivatives have promising applications in many biological fields, including cell culture, drug delivery, and tissue engineering. Although these hydrogels have been widely reported to have low cytotoxicity, biocompatibility, and tunable bioactivity, problems such as harsh preparation conditions and complex material design hinder their application. Herein, by adjusting pH to induce non-covalent interactions between small-molecule tryptophan derivatives (*N*-[(phenylmethoxy)carbonyl]-L-tryptophan, Mw: 338.35), we developed a self-assembled three-dimensional network hydrogel that can be rapidly formed in seconds. And the supramolecular self-assembly mechanism of the hydrogels was also investigated in detail through experimental characterizations and density functional theory calculation. As-prepared hydrogels also exhibit reversible pH-stimulated response and self-healing properties. This study details a research process for the simple and rapid preparation of tryptophan derivative-based hydrogels, which provides more reference ideas for the future development of materials based on other amino acid derivatives.

Small-molecule hydrogels based on amino acid derivatives have received extensive attention in recent years, occupying an indispensable position in biology and material arrays, such as cell culture, drug delivery and tissue engineering and other fields [1–4]. In contrast to most polymers, these hydrogels typically have supramolecular networks composed of ordered, regular, and repetitive building blocks, which are particularly important for studying the gelling mechanism. Most of them are widely available, simple, versatile and useful self-assembled building blocks, including acceptors and donors. In addition, amino acids are cheap and widely available, and most of the hydrogels prepared from amino acid derivatives have high water content, diversity and utilization [5–8]. More importantly, this highly biocompatible hydrogel can not only provide an optimal moist environment for physiological conditions to promote wound healing, but also play a unique curative effect by blending with other drugs or grafting special groups [9–11].

The physical and physiological performance of amino acid derivatives hydrogels often originate from the property of their functional groups. This leads to the fact that the preparation process of traditional solid-phase peptide synthesis not only requires precise design of multiple amino acid combinations, but also involves multiple steps and complicated procedures [12–14]. In addition, some short peptides synthesized from amino acids require additional additives (metal ions, polymers), as well as sufficient gel formation conditions (light time, temperature). Certain synthetic additives may cause side effects such as inflammation, immunogenic and oxidative DNA damage, and concerns about degradability or toxicity [15–17]. In recent years, more and more attention has been paid to developing safe and rapidly prepared hydrogels. Especially in emergency situations, after the injured part forms a hydrogel protective layer faster, it can be isolated from the outside world in time, and the moist environment of the wound can be maintained to avoid bacterial infection. The formed gel can also release the corresponding drugs, thereby realizing various physio-

* Corresponding authors.
E-mail addresses: dengchunyan@csu.edu.cn (C. Deng), yzhangcsu@csu.edu.cn (Y. Zhang).
[1] These authors contributed equally to this work.

https://doi.org/10.1016/j.cclet.2022.108069
1001-8417/

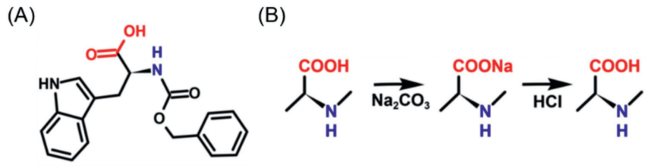

Scheme 1. (A) Molecular structure of **ZW** and (B) pH regulation process.

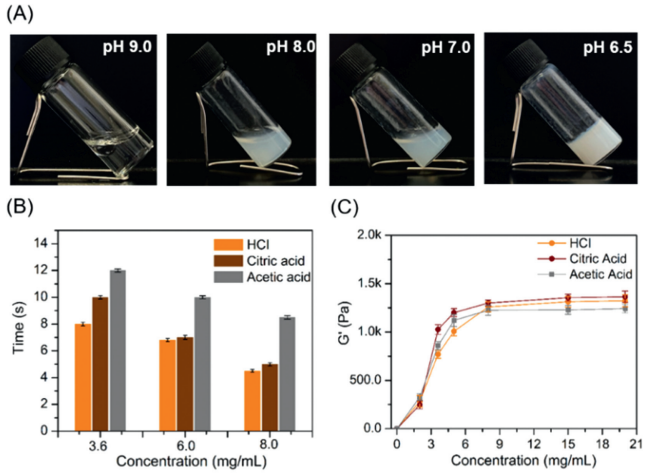

Fig. 1. (A) Photographs of **ZW** solutions at different pH conditions. (B) gelation time and (C) storage modulus *G'* of hydrogels conditioned with different acids.

logical functions such as rapid hemostasis and pain relief [18–20]. Furthermore, reducing the requirements for process conditions and shortening the lengthy preparation process will further expand the application range of gels, which is conducive to the large-scale production of functional gels. Therefore, amino acid derivative hydrogels are the main carriers of most drugs, and it is particularly important to explore safe and fast preparation methods.

It has been reported that many amino acid derivatives with aromatic rings can also form hydrogels through non-covalent forces [21–24]. In some self-assembled hydrogels of small molecules, strong π-π stacking and hydrophobic interactions exist between cyclic conjugated systems such as benzene, naphthalene, and anthracene [25–27]. In addition, the formation of the ordered structure of self-assembled hydrogels is the result of the synergistic effect of various non-covalent bonds between molecules, and hydrogen bonds are also an important intermolecular force that forms the gelation process [28–31]. These non-covalent forces are important driving forces for the self-assembly of network fibers to form hydrogels.

Based on these theoretical foundations, we explored a common small molecule of tryptophan derivatives, namely *N*-[(phenylmethoxy)carbonyl]-L-tryptophan (**ZW**, Z stands for benzene ring, W stands for tryptophan, Mw: 338.35), and found that it has the property of rapid gelation. Usually, it is widely used as an intermediate for synthetic raw materials and pharmaceuticals, like most amino acids with protective groups. Therefore, its potential properties have not been fully reported. Notably, **ZW** was not soluble in ordinary deionized water and did not change significantly even when heated to 80 °C (Fig. S1 in Supporting information). While it can be dissolved in alkaline solution in the form of salt and dispersed uniformly. By adding the acid to the solution, the molecule will return to its original shape (Scheme 1). Due to the presence of groups such as benzene rings and carboxyl groups in the structure, self-assembly behaviors based on π-π stacking and hydrogen bonding may occur in this process.

The preparation process is shown schematically in Fig. 1A. First, 30.0 mg **ZW** powder was dissolved in Na_2CO_3 solution by ultrasonic treatment to obtain 5 mL colorless and transparent solution. Then 0.05 mL of HCl solution (0.1 mol/mL) was gradually added dropwise, and the pH and morphological changes of the material were monitored. Meanwhile, invert the tube to confirm gelation. Initially, the solution did not produce a clear precipitate, but a milky white suspension. Interestingly, the **ZW** solution rapidly gelled when adjusted to pH 6.5. When pH was changed from 6.5 to 3.0, the hydrogel changed from a translucent state to eventually a white and fully opaque hydrogel. The appearance of the **ZW** hydrogel did not change significantly after pH was lower than 3.0. In addition, it is also proved that 3.6 mg/mL is the lowest gel-forming concentration (Fig. S2 in Supporting information), and the *G'* (storage modulus) of hydrogel samples is always greater than *G"* (loss modulus), indicating the elastic properties of this hydrogel (Fig. S3 in Supporting information).

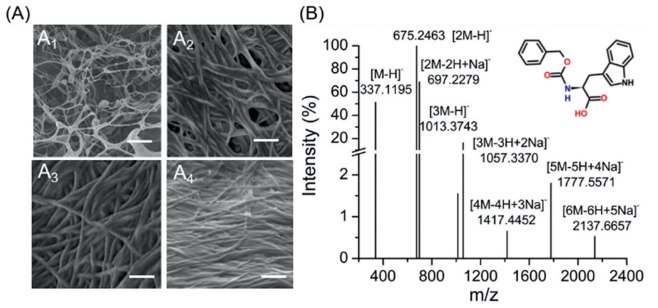

Fig. 2. (A) SEM images of the **ZW** hydrogel at (A1) pH 7.0, (A2) pH 6.5, (A3) pH 5.0, and (A4) pH 3.0, scale bar: 100 nm. (B) Mass spectra of the **ZW** hydrogel.

Subsequently, common citric acid and acetic acid were also used to test the sol-gel transition with different concentrations (Fig. 1B). Both of them were made into a 0.1 mol/mL solution, and then gradually added to 0.15 mL, and compared with HCl. As shown in Fig. 1B, with the increase of the concentration of **ZW** solution, the gel formation time is significantly reduced. Especially after the addition of HCl and citric acid, the gel can be rapidly formed within 10 s. The reason for the slow rate of acetic acid forming a gel may be that the acidification of the weak acid takes a period of time. It can be seen that after the addition of citric acid, the *G'* value of the **ZW** hydrogel is the highest among the three acids (Fig. 1C), even reaching 1260 Pa. It is noted that after the concentration reaches 6.0 mg/mL, the *G'* value is basically unchanged, indicating that the self-assembly of the molecule has reached saturation. These results are beneficial to making the hydrogel more convenient by adjusting the concentration and the type of acid, and the preparation process of the hydrogel is very simple and easy to form.

Scanning electron microscopy (SEM) images showed that the scaffold of the **ZW** hydrogel (6 mg/mL) at pH 3.0–7.0 was a 3D interconnected network composed of nanofibers with diameters of 40–80 nm (Fig. 2A), while the **ZW** solution at pH 9.0 showed no obvious fibrous structure but only irregular granular (Fig. S4 in Supporting information) [32]. The structure formed at pH 6.5 showed several long fibers with diameters of approximately 40–60 nm and lengths greater than 500 nm overlapping each other, forming a distinctly cross-linked fiber network. These results suggest an adjustment of pH can achieve solution gelation of **ZW** hydrogels.

To investigate the self-assemble mechanism of the hydrogel, mass spectrometer (MS) was applied to analyze aggregate structures. As shown in Fig. 2B, in negative ion mode (*m/z* 200–2400), the mass spectrometer detected monomer (*m/z* 337.1195), dimer (*m/z* 675.2463 and 697.2279), trimer (*m/z* 1013.3743 and 1057.3370), tetramer (*m/z* 1417.4452), pentamer (*m/z* 1777.5571) and higher-order aggregates were detected in the ESI-MS spectra of nanofibrils. In the complete mass spectrum (Fig. S5 in Support-

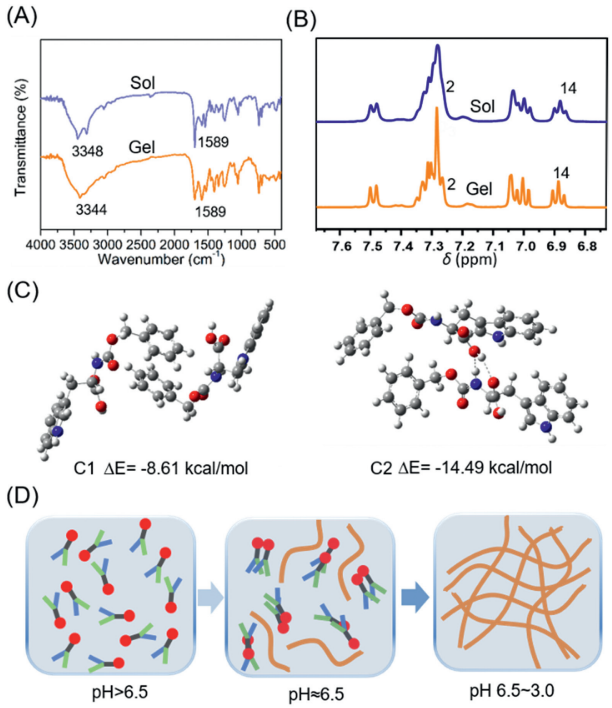

Fig. 3. (A) FT-IR spectra and (B) ^{1}H NMR spectra of **ZW** solution and **ZW** hydrogel. The concentration was 6 mg/mL. (C) Possible structures and interaction energies of **ZW** dimers. (D) Possible process of hydrogel formation during pH adjustment.

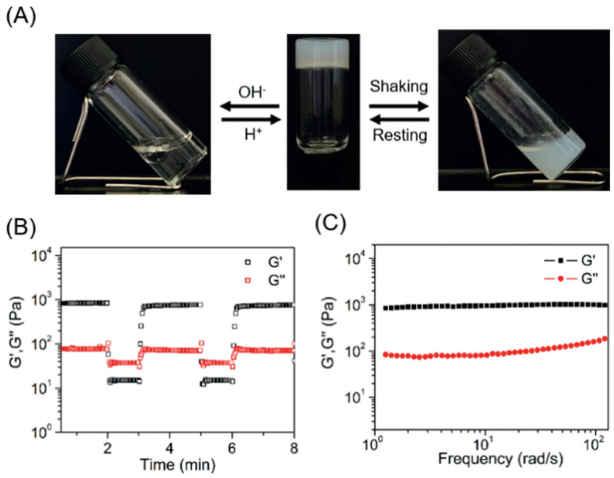

Fig. 4. (A) Photographs of **ZW** hydrogel preparation in a common centrifuge tube. (B) Alternate step-strain sweep measurements with high strain (100%) to low strain (0.1%) for five cycles. (C) Dynamic frequency sweep of the hydrogel with a fixed strain (0.1%).

ing information), there are some fragment ion peaks in addition to the molecular ion peak. The relative content of dimer was consistently highest, indicating that is more stable than other aggregates and is not easily broken by the ion source. It can be speculated from the above that a three-dimensional network of **ZW** hydrogels is composed of nanofibers, which in turn are formed by continuous aggregation of **ZW** monomers.

Further characterizations were carried out to investigate the driving force of the **ZW** molecules to form hydrogels. As shown in Fig. 3A, the stretching vibration peak belonging to O–H/N–H shifted from 3348 cm^{-1} to 3344 cm^{-1} during the sol-gel transition. The shift of the IR absorption bands to lower wavenumbers suggested the existence of stronger hydrogen bonds during the self-assembly process [33–35]. Moreover, the vibration associated with the carboxyl group at 1589 cm^{-1} was enhanced after self-assembly, indicating that the carboxyl and ester groups of the molecule may be involved in the formation of hydrogen bonds.

The driving force of **ZW** molecular aggregation was further investigated by ^{1}H NMR. The vicinal proton-proton coupling relationship was first recorded by 2D ^{1}H-^{1}H–COSY NMR to determine the chemical shift of each proton of the structure (Figs. S6 and S7 in Supporting information). Notably, the hydrogens of the secondary amides (-NH-marked 14) on the solution clearly shifted downfield, from δ 6.37 to δ 6.48 (Fig. 3B). It has been reported that after the molecule forms hydrogen bonds, the density of the electron cloud around the hydrogen nucleus decreases, resulting in a deshielding effect [36–38]. The shielding effect of hydrogen-bonded protons is smaller than that of non-hydrogen-bonded protons, so resonances occur at low fields with larger δ values. This illustrates the formation of obvious hydrogen bonds between -NH- on the structure and other groups. In addition, the aromatic proton signal (marked 2) attributed to the benzene ring exhibits a distinct change and begins to shift downfield from the position of δ 7.25 to δ 7.35, indicating intermolecular generated π-π interactions.

Intermolecular π-π stacking and hydrogen bonding interactions are the two driving forces for the formation of hydrogels, and stable dimers may be the key to the rapid gelation of such small molecules. Considering the nature of the molecular structure, the possible **ZW** dimer structure was further deduced by density functional theory (DFT). As shown in Fig. 3C, the structure C1 is formed by π-π stacking of benzene rings, and C2 is formed by hydrogen bonding of secondary amino groups (-NH-) and carbonyl groups (C=O). By further calculation, the interaction energies of C2 have the lowest binding energy (−14.49 kcal/mol), indicating that the formation of hydrogen bonds may be more conducive to the stability of the structure [39–41]. In addition, among other possible structures, the binding energy of the hydrogen-bonding-based dimer is also lower than that of the indole ring-based π-π stacking (Fig. S8 in Supporting information). The interaction energies of these structures are mostly below −7.0 kcal/mol, and one or several of them may be involved in the formation of **ZW** fibers in the sol-gel transition (Fig. 3D). Furthermore, dimers are relatively easy to form in water, and the two molecules have already presented an obvious dimer form at 45 ns (Fig. S9 in Supporting information). It is possible that dimers or multimers determine the chemical properties and biological activities of **ZW** hydrogels, which need to be further explored in the future.

The reversible breaking and reformation of π-π stacking and hydrogen bonds generally can endow gels with self-healing properties. It is found that the gel will turn into a solution after adding Na_2CO_3 solution, and the gel can still be formed quickly by adding HCl again. Additionally, the conversion can also be achieved by shaking tests. When the hydrogel was shaken vigorously and turned into a sol, it could be recovered after standing for a few minutes (Fig. 4A). Further rheological tests were performed to verify the performance of the hydrogel. Experiments show that the **ZW** hydrogel will undergo an obvious gel-sol transition when the strain is higher than 19.8% (Fig. S10 in Supporting information). In the gel state, at a small strain of 0.1%, *G*' is greater than *G*" (Fig. 4B). When the strain is increased to 100%, the *G*' and *G*" values reverse, indicating the formation of a sol state. When 0.1% strain was applied again, the *G*' value became higher than the *G*" value in about 5 s. The repeatability of this gel-sol was confirmed in three cycles. Reducing the strain ($\gamma = 0.1\%$, frequency = 0.5 Hz) after the rapid recovery of *G*' and *G*" indicates reorganization of the gel structure. This rapid destruction-formation process also proves that the sol-gel is very easy to form with obvious self-healing properties. Moreover, dynamic frequency sweeps indicated that *G*' was 10 times

larger than *G*", showing a weaker frequency dependence in this range (Fig. 4C). It is worth noting that the carboxyl and secondary amino groups in the molecular structure are easy to form strong coordination bond with metal ions, which may destroy the hydrogen bonds of the gel structure itself. The experiment also proved that the addition of the latter obviously led to the precipitation of the system (Fig. S11 in Supporting information).

What is more, good biocompatibility is the prerequisite for biomedicine application of the material. The CCK-8 assay was used to evaluate cell toxicity of the hydrogel and analyze the influence of different **ZW** concentrations on cell viability [42,43]. After incubating the solution and hydrogel with L929 fibroblasts for 24 h, cell viability was assessed by CCK-8 reagent. Compared with the control group, the hydrogels induced no significant cytotoxic effect at 8 mg/mL (Fig. S12 in Supporting information), indicating that this hydrogel material possessed high biocompatibility that offered an important foundation for its biological research. Therefore, this simple condition and rapid process of **ZW** hydrogel with excellent thixotropic is promising as an injectable biomedical material for drug delivery and release.

In conclusion, we developed a tryptophan derivative small-molecule hydrogel with protective groups. By adjusting the pH of the solution, hydrogels can be rapidly prepared within seconds. Experimental characterization and theoretical calculations demonstrate that intermolecular hydrogen bonds and π-π stacking of aromatic rings are the main driving forces for gel formation. Experiments further proved that the material has self-healing properties and good compatibility with normal mammalian cells. The results may contribute to the development and utilization of amino acid derivatives, and also provide valuable ideas for exploring the rapid preparation of small molecule hydrogels.

Declaration of competing interest

The authors declare that they have no known competing financial interests or personal relationships that could have appeared to influence the work reported in this paper.

Acknowledgments

This work was financially supported by the National Natural Science Foundation of China (Nos. 21773311 and 21972169), and Hunan Provincial Science and Technology Plan Project (No. 2017TP1001). Thanks for the software support provided by the High Performance Computing Center of CSU and NMR data support provided by the Institute of Chemistry Chinese Academy of Sciences.

Supplementary materials

Supplementary material associated with this article can be found, in the online version, at doi:10.1016/j.cclet.2022.108069.

References

[1] K. Hawkins, A.K. Patterson, P.A. Clarke, D.K. Smith, J. Am. Chem. Soc. 142 (2020) 4379–4389.
[2] R. Marti-Centelles, J. Rubio-Magnieto, B. Escuder, Chem. Commun. 56 (2020) 14487–14490.
[3] C.C. Piras, C.S. Mahon, D.K. Smith, Chemistry (Easton) 26 (2020) 8452–8457.
[4] C.C. Piras, P. Slavik, D.K. Smith, Angew. Chem. Int. Ed. 59 (2020) 853–859.
[5] S. Wu, Q. Zhang, Y. Deng, et al., J. Am. Chem. Soc. 142 (2020) 448–455.
[6] X. Zhao, H. Zhang, Y. Gao, et al., ACS Appl. Bio. Mater. 3 (2020) 648–653.
[7] Q. Chen, L. Cui, Y. Guan, Y. Zhang, Biomacromolecules 22 (2021) 3474–3485.
[8] E.R. Cross, S.M. Coulter, S. Pentlavalli, G. Laverty, Soft Matter 17 (2021) 8001–8021.
[9] Y. Li, M.J. Mannel, N. Hauck, et al., Angew. Chem. Int. Ed. 60 (2021) 6724–6732.
[10] S. Pal, V. Soni, S. Kumar, et al., Nanoscale 13 (2021) 13225–13230.
[11] Y. Zhang, Y. Ding, X. Li, et al., Chin. Chem. Lett. 32 (2021) 3636–3640.
[12] L. Cai, S. Liu, J. Guo, Y.G. Jia, Acta Biomater. 113 (2020) 84–100.
[13] M. Gomez-Florit, A. Pardo, R.M.A. Domingues, et al., Molecules 25 (2020) 5858.
[14] S.D. Bhagat, A. Chanchal, M. Gujrati, et al., Biomater. Sci. 9 (2021) 261–271.
[15] L. Dong, H. Chen, T. Liu, et al., Biomacromolecules 22 (2021) 5374–5381.
[16] L. Wang, J. Li, Y. Xiong, et al., ACS Appl. Mater. Interfaces 13 (2021) 58329–58339.
[17] M. Gharakhloo, D. Jagleniec, J. Romanski, M. Karbarz, J. Mater. Chem. B 10 (2022) 4463–4472.
[18] M.S. Liberato, N.G.S. Cavalcante, P.A. Sindu, et al., Soft Matter 17 (2021) 10926–10934.
[19] N. Maldonado, P. Amo-Ochoa, Nanomaterials 11 (2021) 1865.
[20] J. Rickhoff, N.V. Cornelissen, T. Beuse, et al., Chem. Commun. 57 (2021) 5913–5916.
[21] M. Muhammad, C. Willems, J. Rodriguez-Fernandez, et al., Biomolecules 10 (2020) 1185.
[22] S.S.S. Aye, Z.H. Zhang, X. Yu, et al., ACS Biomater. Sci. Eng. 8 (2022) 89–99.
[23] C. Wang, Y. Liu, X. Qu, et al., Adv. Mater. 34 (2022) e2105416.
[24] X.Q. Wang, K.H. Chan, W. Lu, et al., Nat. Commun. 13 (2022) 3369.
[25] Z. Sun, Z. Li, Y. He, et al., J. Am. Chem. Soc. 135 (2013) 13379–13386.
[26] X. Wang, T. He, L. Yang, et al., Nanoscale 8 (2016) 6479–6483.
[27] J. Zheng, R. Fan, H. Wu, et al., Nat. Commun. 10 (2019) 1604.
[28] A.D. Shaller, W. Wang, H. Gan, A.D. Li, Angew. Chem. Int. Ed. 47 (2008) 7705–7709.
[29] E.L. Bakota, O. Sensoy, B. Ozgur, et al., Biomacromolecules 14 (2013) 1370–1378.
[30] A. Osypenko, E. Moulin, O. Gavat, et al., Chemistry (Easton) 25 (2019) 13008–13016.
[31] X. Song, Z. Zhang, Z. Shen, et al., ACS Appl. Mater. Interfaces 13 (2021) 56881–56891.
[32] Y. Sun, X. Li, M. Zhao, et al., Bioact. Mater. 8 (2022) 396–408.
[33] G. Bastiat, J.C. Leroux, J. Mater. Chem. 19 (2009) 3867–3877.
[34] T. Figueiredo, V. Cosenza, Y. Ogawa, et al., Soft Matter 16 (2020) 3628–3641.
[35] Z. Meng, Y. He, F. Wang, et al., ACS Appl. Bio. Mater. 4 (2021) 2713–2722.
[36] S. Mandal, S. Hait, F. Simon, et al., ACS Appl. Polym. Mater. 4 (2022) 6612–6622.
[37] F. Muscas, V. Sessini, L. Peponi, et al., Polymers (Basel) 14 (2022) 3447.
[38] H.L. Yang, H.T. Lu, Y.Y. Miao, et al., Chem. Eng. J. 450 (2022) 138346.
[39] M. Anza, M. Endale, L. Cardona, et al., Adv. Appl. Bioinform. Chem. 14 (2021) 117–132.
[40] A.M. Garcia, M. Melchionna, O. Bellotto, et al., ACS Nano 15 (2021) 3015–3025.
[41] X. Lin, M. Fang, C. Yi, et al., Biomaterials 280 (2022) 121278.
[42] P.J. Jervis, L. Hilliou, R.B. Pereira, et al., Nanomaterials 11 (2021) 704.
[43] C.B.P. Oliveira, S.R.S. Veloso, E.M.S. Castanheira, et al., Soft Matter 18 (2022) 3955–3966.